Available online at www.sciencedirect.com
SCIENCE DIRECT
Journal of Catalysis 228 (2004) 80–91
JOURNAL OF CATALYSIS
www.elsevier.com/locate/jcat

$Ag–SiO_2–Al_2O_3$ composite as highly active catalyst for the formation of formaldehyde from the partial oxidation of methanol

Wei-Lin Dai [a,*], Yong Cao [a], Li-Ping Ren [a], Xin-Li Yang [a], Jian-Hua Xu [a], He-Xing Li [b], He-Yong He [a], Kang-Nian Fan [a]

[a] *Department of Chemistry and Shanghai Key Laboratory of Molecular Catalysis and Innovative Materials, Fudan University, Shanghai 200433, People's Republic of China*

[b] *Department of Chemistry, Shanghai Normal University, Shanghai 200234, People's Republic of China*

Received 1 July 2004; revised 21 August 2004; accepted 24 August 2004

Available online 22 September 2004

Abstract

Catalytic oxidative dehydrogenation of methanol to formaldehyde was carried out over $Ag–SiO_2–Al_2O_3$ catalysts prepared by a sol–gel method. Detailed preparation conditions were investigated and the optimal preparation parameters were determined as the Si/Al molar ratio of 8.5/1.5–9/1, silver loading of 20 wt%, and calcination temperature of 900–1000 °C with ethanol as the solvent. Under optimum reaction conditions, i.e., the reaction temperature of 640 °C, O_2/CH_3OH molar ratio of 0.39 with space velocity (GHSV) of 1.2×10^5 h^{-1}, the as-prepared catalyst exhibits excellent activity and selectivity. The yield of formaldehyde reaches 91%, much higher than that obtained over the pumice-supported silver catalyst (75%) and even higher than that over the commercial electrolytic silver catalyst (85%). Based on combined characterizations, such as X-ray photoelectron spectroscopy and X-ray-excited Auger electron spectroscopy (XPS and XAES), nitrogen adsorption at low temperature, thermogravimetry and differential thermogravimetry (TG-DTG), differential thermal analysis (DTA), diffuse reflectance ultraviolet visible spectroscopy (UV–vis DRS), temperature-programmed reduction (TPR), scanning electron micrograph (SEM), X-ray diffraction (XRD), etc., the correlation of the catalytic performance to the structural properties of the $Ag–SiO_2–Al_2O_3$ catalyst is discussed in detail. It is found that almost all the catalysts are glass-like and nonporous with a surface area of ~ 1 m^2/g. In the catalysts with silver loading lower than 20 wt%, all the silver species are present as Ag^+ ions before the reaction and the catalyst is ultrathermally stable even under elevated temperatures at 1100 °C owing to the stabilizing effect of the $[AlO_4]$ group. Higher Ag loading in the catalysts leads to the presence of metallic silver species over the surface of the catalyst. During the catalytic reaction, Ag^+ ions are partially reduced to metallic Ag. These nano-sized Ag particles act as the active centers and the superior catalytic performance of the $Ag–SiO_2–Al_2O_3$ catalyst is attributed to its unique surface structure and the strong interactions between the support and the active phase.

Keywords: Supported silver catalyst; Formaldehyde; Methanol oxidation; Sol–gel method; X-ray photoelectron spectroscopy

1. Introduction

Formaldehyde, with an annual production up to $4–5 \times 10^7$ tons, is mainly commercially produced from methanol oxidation over silver-based catalysts [1]. Owing to such large production scale, there is a strong driving force to develop new catalysts and to optimize the reaction conditions [2–6] since a very little improvement may bring about great economic benefits. It is known that the methanol-rich process using the silver-based catalyst is a preferred route owing to its moderate operating conditions and simplicity of reactor design in comparison with the oxygen-rich process using iron–molybdate catalysts [2]. Currently, the dominant commercial Ag catalyst used throughout the world in the methanol oxidation process is electrolytic silver. However, the short lifetime ($\sim$ 3–6 months) of the electrolytic silver strongly restricts its wide use in industry and results in the relatively high price of formaldehyde [7]. Although the pumice-supported Ag catalysts exhibits a much longer

* Corresponding author. Fax: +86 21 65642978.
E-mail address: wldai@fudan.edu.cn (W.-L. Dai).

0021-9517/$ – see front matter
doi:10.1016/j.jcat.2004.08.035

lifetime, the potential application of this catalyst system is greatly hampered by its low formaldehyde yield (∼ 75%) in the commercial methanol oxidation process. Consequently, a great number of attempts have been made to develop new supported Ag catalysts with both a long lifetime and a high catalytic efficiency. Among various supported catalysts, the silica–alumina-supported catalysts has attracted particularly interest recently due to their much higher catalytic activity even at a substantially lower Ag loading than pumice-supported Ag catalyst (40 wt% silver content). However, these silica–alumina supports are mainly obtained by thermal treatment of various materials used in ceramic production [8,9] and the preparation process of such supported catalysts is rather complicated.

Recently, the sol–gel method has attracted much attention by providing a new approach to preparing highly dispersed supported catalysts, which may even have excellent resistance to sintering [10–12]. Our previous work showed that the novel Ag–SiO_2–Al_2O_3 catalyst system prepared by the sol–gel method followed by a high-temperature calcination exhibited excellent activity and selectivity in the selective oxidation of methanol to formaldehyde [13,14]. The yield of formaldehyde reached 91% and the conversion of methanol was near 98%. However, our previous work only reported the preliminary preparation method and reaction conditions as well as some related characterization results. In order to gain a fundamental understanding of the nature as well as the catalytic performance of this novel catalyst system, much detailed study should be carried out. In this paper, the novel Ag–SiO_2–Al_2O_3 catalyst system is extensively studied in its preparation and characterization with TG-DTG, DTA, XRD, SEM, UV–vis DRS, TPR, XPS, etc. A reasonable correlation of the structural parameters with its catalytic activity is also proposed.

2. Experimental

2.1. Catalyst preparation

The Ag–SiO_2–Al_2O_3 sol–gel composites were prepared from the precursors of $Si(OC_2H_5)_4$ (TEOS), $Al(NO_3)_3 \cdot 9H_2O$, and $AgNO_3$. A typical procedure is as follows: 67 mL of TEOS was mixed with 2 mL of 0.1 M HNO_3 in 50 mL ethanol at 70 °C for 1.0 h to obtain a silica sol solution. The solution was refluxed with a magnetic stirrer at 70 °C for another 2.0 h, and then an aqueous solution containing 7.36 g $Al(NO_3)_3 \cdot 9H_2O$ and 50 mL distilled water was added. The resulting mixture was stirred at 75 °C for an additional 12 h. Finally, the resultant gel was dried at 120 °C overnight followed by calcination at 900 °C in air for 10 h. The as-prepared sample was colorless and transparent and was grounded to grain sizes of 40–60 mesh for the activity test.

2.2. Characterization and activity test

Porosity was determined from N_2 adsorption isotherms at −196 °C by using Micromeritics Tristar 3000 apparatus. TG-DTG and DTA were recorded on a Perkin–Elmer 7 thermal analyzer. XRD patterns were recorded on a Bruker D8 advance diffractometer at 2θ range of 10–90° with Cu$K\alpha$ radiation. SEM was performed on a Philips XL30 scanning electron micrograph. XPS experiments were carried out with a Perkin–Elmer PHI 5000C ESCA system using Al$K\alpha$ radiation (1486.6 eV) at a power of 250 W. The pass energy was set as 93.9 eV and the binding energies were calibrated by using contaminant carbon at BE of 284.6 eV. The UV–vis DRS spectra were obtained on a Hitachi UV-330 spectrometer. FTIR spectra were recorded with a Nicolet 5SDX spectrometer and FT-Raman experiments were performed with a Perkin–Elmer Spectrum 2000 NIR spectrometer. TPR experiments were carried out in a set of homemade equipment.

The catalytic oxidation of methanol over the novel Ag–SiO_2–Al_2O_3 sol–gel composite was carried out in a flow-type quartz reactor (i.d. = 16 mm) at a reaction temperature range of 550–700 °C with a GHSV of $1.2 \times 10^5\ h^{-1}$. An aqueous solution of methanol (60 wt%) was pumped into the evaporator kept at 220 °C and then fed into the reactor after being mixed with air. Gaseous products (H_2, CO, CO_2, etc.) and formaldehyde in solution were analyzed by using online gas chromatography (GC) analysis and chemical titration, respectively. The standard deviation of the values of methanol conversion as well as the HCHO yield were ±0.2%, while that of the yield of ($CO + CO_2$) was ±0.5%. The carbon balance was tested as 98–102%. Details can be found in our previous works elsewhere [15–17].

3. Results and discussion

3.1. Catalytic activity aest

3.1.1. Effects of preparation parameters

In order to select suitable solvent for the preparation of the catalysts, many kinds of water–alcohol mixed solvents are tested, such as water–ethanol, water–isopropyl alcohol, water–*tert*-butanol, and water–ethylene glycol. It is found that there is little difference among all the mixed alcohol–water solvents. Thus, water–ethanol is chosen as the alcoholic mixed solvent for its convenience and cheapness. One typical catalyst with silver loading of 10%, Si/Al molar ratio of 9/1, and calcination temperature of 1000 °C is chosen to study the effect of the water/ethanol ratio (8, 16, 24, 32, 40, and 48) on the preparation. No appreciable influence of the volume ratio of water/ethanol on the catalytic performance is observed. Given the convenience of usage and the proper time for the sol formation, the volume ratio of water/ethanol is set as 16. By fixing the volume ratio of water/ethanol at 16, silver loading at 10%, Si/Al molar ratio at 9/1, a series of Ag–SiO_2–Al_2O_3 catalysts are prepared to investigate the

Table 1
Influence of the silver loading on the catalytic activity

Silver loading (wt%)	CH_3OH conver. (%)	HCHO yield (%)	$CO + CO_2$ yield (%)
0	87.0	10.2	6.8
0.5	98.2	78.0	7.6
1	99.5	87.0	10.8
2	99.0	87.4	9.2
5	98.0	88.7	9.0
10	98.2	89.1	7.9
20	97.5	89.9	7.5
30	97.2	89.2	8.0
40	97.0	88.6	8.4

Reaction conditions: reaction temperature ∼ 640 °C; O_2/CH_3OH molar ratio ∼ 0.40; GHSV ∼ 1.2×10^5 h^{-1}.

effect of calcination temperatures (from 600 to 1100 °C) on the catalytic activity. As the yield of formaldehyde reaches a maximum value of ∼ 91% in the calcination temperature region of 900–1000 °C, the best calcination temperature is chosen as 900–1000 °C. Also by changing the molar ratio of Si/Al for a given catalyst with silver loading of 20 wt%, water/ethanol of 16 and calcined at 1000 °C, a suitable molar ratio of Si/Al is optimized to be in the range of 8.5/1.5–9/1. As the dope of Al is decreased to zero, the catalytic activity result is similar to that of the Ag/SiO_2 catalyst reported previously [15].

With the optimized preparation conditions being confirmed as water/ethanol of 16, calcination temperature at 1000 °C, and Si/Al molar ratio of 8.5/1.5–9/1, a series of catalysts with different silver loading are prepared and the catalytic activity for the oxidation of methanol to formaldehyde is shown in Table 1. The yield of formaldehyde as a function of silver loading appears as a typical volcano curve. The catalyst with the silver loading at 20 wt% shows the best performance of formaldehyde yield of 89.9%, while both lower and higher silver loadings lead to a decreased formaldehyde yield. It is worthwhile to note that the $Ag–SiO_2–Al_2O_3$ catalyst exhibits a rather high activity (formaldehyde yield is 87.0%) even if the silver loading is as low as 1%, which is already much higher than that of a commercial 40 wt% Ag/pumice catalyst. In addition, the blank test of the support shows extremely low activity, with the main product being dimethylether (DME) (not shown in the table), probably originated from the trace amount of acid sites present on the surface of $SiO_2–Al_2O_3$ supports. This result also unambiguously confirms that the active center for this reaction must be related to the presence of silver. Detailed studies on the characterization of silver on the $SiO_2–Al_2O_3$ supports will be discussed hereinafter. Thus, according to the experimental results discussed above, the most efficient $Ag–SiO_2–Al_2O_3$ catalyst used in the partial oxidation of methanol to formaldehyde is optimized as silver loading of 20 wt%, water/ethanol of 16, and Si/Al of 8.5/1.5–9/1 and is calcined under 900–1000 °C.

3.1.2. Effects of reaction conditions

As previously reported [13], the yield of formaldehyde as a function of the molar ratio of O_2/CH_3OH on the optimal $Ag–SiO_2–Al_2O_3$ catalyst is similar to that obtained on a commercial electrolytic silver catalyst. It is found that the optimal value of O_2/CH_3OH molar ratio over the $Ag–SiO_2–Al_2O_3$ catalyst (0.38–0.39) is only slightly smaller than that over the commercial electrolytic silver catalyst (0.40–0.42), but the catalytic activity of the $Ag–SiO_2–Al_2O_3$ catalyst is much higher than that of the commercial electrolytic silver catalyst at the whole range of the O_2/CH_3OH molar ratios (0.30–0.46). It is also notable that the yield of formaldehyde decreases abruptly with the decrease of the molar ratio of O_2/CH_3OH over the commercial electrolytic silver catalyst, in sharp contrast to the fact that the yield of formaldehyde decreases only very little, regardless of the change of the molar ratio of O_2/CH_3OH, even if the O_2/CH_3OH molar ratio value is as small as 0.35 for the $Ag–SiO_2–Al_2O_3$ catalyst. Therefore, the present novel $Ag–SiO_2–Al_2O_3$ catalyst system shows a particularly attractive potential for practical operation due to its much wider operating range in terms of O_2/CH_3OH molar ratio required for the title reaction.

The influence of reaction temperature on the yield of formaldehyde has been previously reported and a similar behavior as that of the commercial electrolytic silver catalyst was obtained. The optimal reaction temperature of the $Ag–SiO_2–Al_2O_3$ catalyst is found to be 650 °C, only a little higher than that of the commercial electrolytic silver catalyst (630 °C). It is also worthwhile to note that the operation range of reaction temperature of this novel $Ag–SiO_2–Al_2O_3$ catalyst is wider than that of the electrolytic silver catalyst. It is well known that the crystalline silver catalyst may suffer from a rapid deactivation due to sintering at temperatures above 700 °C. However, the present $Ag–SiO_2–Al_2O_3$ catalyst shows excellent thermal stability in terms of sustaining reaction temperatures as high as 1000 °C. Moreover, it is interesting to find that even at low temperatures, such as 500 °C, the $Ag–SiO_2–Al_2O_3$ catalyst still shows high yield of formaldehyde (∼ 85%) while the electrolytic silver counterpart only has a yield of 50%, indicating the novel $Ag–SiO_2–Al_2O_3$ catalyst also has a wide operating range in terms of reaction temperature. Table 2 lists the typical reaction results for the novel $Ag–SiO_2–Al_2O_3$ catalyst and the commercial electrolytic silver under their optimal reaction conditions. It is remarkable that the yield of formaldehyde reaches up to 91% while the yield of CO_2 is only 7% over the $Ag–SiO_2–Al_2O_3$ catalyst, which demonstrates at least two advantages of the catalyst compared with the traditional electrolytic silver. First, the yield of formaldehyde is 6% higher than that of the electrolytic silver, which may result in great economic benefits due to the huge production of formaldehyde all over the world (40–50 million tons per year). Secondly, as the conversion of methanol is rather high (98–99%), the methanol remaining in the product could be achieved at a much lower level thus high-quality formaldehyde can be easily obtained.

Table 2
Catalytic activity results of 20 wt% Ag–SiO_2–Al_2O_3 and electrolytic silver catalysts

Catalyst	Conversion of CH_3OH (%)	Selectivity to HCHO (%)	Yield of HCHO (%)	Yield of ($CO + CO_2$) (%)
Electrolytic silver[a]	93.6	90.2	84.4	9.2
Ag–SiO_2–Al_2O_3[b]	97.8	92.8	90.8	7.0

[a] Reaction conditions: GHSV $\sim 1.2 \times 10^5\ h^{-1}$, reaction temperature $\sim 625\,^\circ C$, $O_2/CH_3OH \sim 0.42$, height of catalytic bed ~ 10 mm, reaction feed ~ 60 wt% aqueous solution of methanol.
[b] Reaction conditions: GHSV $\sim 1.2 \times 10^5\ h^{-1}$, reaction temperature $\sim 635\,^\circ C$, $O_2/CH_3OH \sim 0.39$, height of catalytic bed ~ 10 mm, reaction feed ~ 60 wt% aqueous solution of methanol.

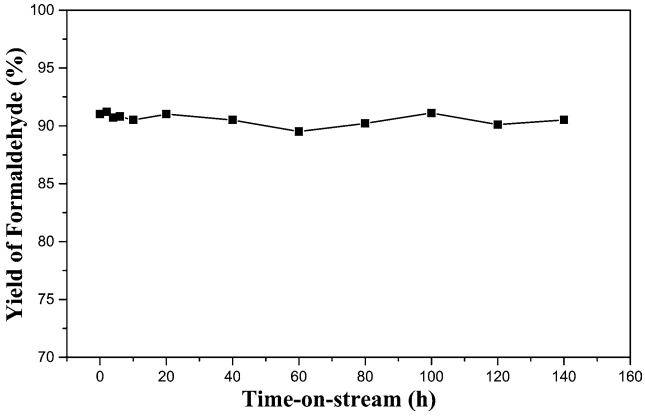

Fig. 1. The lifetime test of the 20 wt% Ag–SiO_2–Al_2O_3 catalyst on the selective oxidation of methanol to formaldehyde.

The lifetime test was carried out in the microreactor. Fig. 1 shows that the Ag–SiO_2–Al_2O_3 catalyst exhibits no appreciable deactivation within 140 h time on stream, which is similar to that of electrolytic silver catalyst. It is generally accepted that the supported catalyst usually has a longer lifetime than the unsupported one, i.e., pumice-supported silver shows 4–5 times longer lifetime than that of electrolytic silver. Although it is not easy to precisely compare the lifetime of both catalysts due to the restriction of experimental conditions for the lifetime test, this result implies that the Ag–SiO_2–Al_2O_3 catalyst may have a much longer lifetime than the commercial electrolytic silver catalyst. Moreover, a 20 wt% Ag–SiO_2–Al_2O_3 catalyst has been operated in an industrial plant (2000 g catalyst, 37% formaldehyde, 20,000 tons per year) by using a lateral-line pilot system with the reactor diameter of 180 mm, showing better performance than the commercial electrolytic silver. During the test period ($\sim$ 10 days), no deactivation was observed. One important character of this novel catalyst system is that this catalyst is much more thermally stable than its commercial polycrystalline silver counterpart, which will be discussed in detail in the characterization section of the present work. Another merit of this catalyst is its good recyclability, as the used catalyst can be easily regenerated to its fresh state with a high-temperature treatment in the presence of pure oxygen or air. In contrast, the polycrystalline one can only be recycled by a complicated reelectrolysis process, which is relatively expensive and inconvenient.

3.2. Characterizations

3.2.1. Specific surface area

Table 3 shows that the specific surface area of all the present Ag–SiO_2–Al_2O_3 catalysts with different silver content is very low (about 1–3 m^2/g), which is considered to be very suitable for the manufacture of formaldehyde from the partial oxidation of methanol [1]. To confirm the detrimental effect of the high surface area to this reaction, a number of Ag–SiO_2–Al_2O_3 catalysts with relatively larger surface areas ($> 10\ m^2/g$) have been prepared. The results show that these catalysts with relatively higher surface areas only exhibit very poor selectivity toward the formation of formaldehyde, possibly due to a further decomposition of formaldehyde on the porous supports.

3.2.2. TG-DTG and DTA

Fig. 2 illustrates TG-DTG and DTA curves of the 20 wt% Ag–SiO_2–Al_2O_3 catalyst. It is obvious that there are two weight-loss processes in the temperature range from 50 to 1000 °C. The first one is located at 77.5 °C, corresponding to the loss of the solvent (ethanol), and the another is very broad in the range of 200–500 °C, which can be ascribed to the weight loss due to the dehydration of the xerogel and the subsequent decomposition of $AgNO_3$. No other obvious changes are observed during the further heating treatment from 600 to 1000 °C, revealing that this catalyst is extremely thermally stable. DTA results are well consistent with the TG-DTG ones. As we know, due to the low thermal stability, the commercial polycrystalline silver catalyst may sinter and result in deactivation if the reaction temperature exceeds 720 °C. However, this will not be the case over the Ag–SiO_2–Al_2O_3 catalyst since it has an extremely higher thermal stability.

Table 3
Specific surface area of the Ag–SiO_2–Al_2O_3 catalysts with different Ag loadings

Silver loading (wt%)	0.5	1	2	5	10	20	30	40
Specific surface area (m^2/g)	1.8	1.0	1.1	3.0	0.9	0.7	1.6	0.9

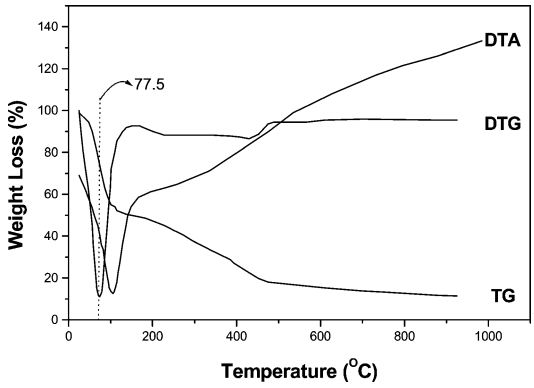

Fig. 2. TG-DTG and DTA curves of the 20 wt% Ag–SiO_2–Al_2O_3 catalyst.

3.2.3. FTIR and Raman spectroscopies

The FTIR spectra of the Ag–SiO_2–Al_2O_3 composite with high Si/Al ratios are very similar to those of amorphous silica. In the 400–1500 cm^{-1} range, only three peaks located at about 470, 785, and 1100 cm^{-1} could be observed, which might be ascribed to vibrations from –O–Si–O^-, Si–O–, and Si–O, respectively. It is clear that the peak positions are slightly different from those of Ag/SiO_2 catalyst that are located at 456, 802, and 1084 cm^{-1}, indicating the modified structure of the Ag–SiO_2–Al_2O_3 catalyst as compared with that of Ag/SiO_2 [15]. Moreover, the bands corresponding to silica–O and cristobalite (low syn) centered at 602 and 693 cm^{-1}, respectively, appearing in the Ag/SiO_2 catalyst are not identified in the Ag–SiO_2–Al_2O_3 sample, suggesting the absence of such phases in Ag–SiO_2–Al_2O_3. In addition, the signals of three characteristic peaks of the Ag–SiO_2–Al_2O_3 catalyst are strongly attenuated and finally disappear with decreasing of the Si/Al ratio, implying that an excessive content of alumina will result in the destruction of the special structure of the Ag–SiO_2–Al_2O_3 catalyst. FT-Raman study also gives similar results as FTIR and there are no Raman bands corresponding to Ag–O vibrations, suggesting that silver does not present as silver oxides in our Ag–SiO_2–Al_2O_3 composite.

3.2.4. XRD

XRD patterns of the Ag–SiO_2–Al_2O_3 catalysts with silver loading ranging from 2 to 40 wt% were reported in our previous work [13]. No sharp peaks are identified for the catalyst with silver loading lower than 20 wt%. However, the characteristic diffraction peaks ascribed to the crystalline Ag(111) (38.1°), Ag(200) (44.3°), Ag(220) (64.4°), and Ag(311) (77.5°) appear in the XRD patterns when silver loading is higher than 20% [15], suggesting the presence of metallic silver particles in the Ag–SiO_2–Al_2O_3 sol–gel composites. In addition, two peaks (21.9 and 36.1°) ascribed to cristobalite (low syn) are also observed, implying that an unusual crystallization of the amorphous silica occurred at a much lower temperature than that required in the absence of silver [18]. On the other hand, no crystalline alumina phase is observed, suggesting that alumina is presented as an amorphous state. In addition, the XRD patterns are only slightly modified with increasing calcination temperature except for that under 1000 °C for 24 h, which shows the formation of a small amount of crystalline cristobalite. Further calcination of the Ag–SiO_2–Al_2O_3 catalyst at 1100 °C for 4 h also results in no appreciable changes of the XRD patterns, which demonstrates its ultrahigh thermal stability and agrees well with the results of thermal analysis. Moreover, changing the molar ratio of Si/Al from 9/1 to 3/7 also does not result in a significant difference in the XRD patterns. However, for the 20 wt% Ag–SiO_2–Al_2O_3 samples, if the Si/Al ratio is increased from 9/1 to $\propto$, crystalline silver phases appear.

Another interesting point is that there is a remarkable difference for the catalyst with silver loading lower than 20 wt% before and after reaction for 2 h. As previously reported, the typical XRD peaks of the 20 wt% Ag–SiO_2–Al_2O_3 catalyst after reaction for 2 h are rather similar to those with silver loadings higher than 20 wt%, indicating that Ag^+ in the Ag–SiO_2–Al_2O_3 catalyst is reduced to metallic silver during the reaction of the selective oxidation of methanol. The XRD patterns for the used catalyst (> 100 h) and the one after reaction for 2 h are almost the same, suggesting that the crystalline structure is retained during the reaction after the induction period. This result also implies that the active centers for this reaction might be associated with the metallic silver particles owing to the fact that there are crystalline silver phases appearing in the process of the reaction, which agrees very well with that from the SEM data discussed as follows.

3.2.5. SEM

Fig. 3 shows the SEM micrographs of 10, 20, and 30 wt% Ag–SiO_2–Al_2O_3 catalyst before and after reaction for 2 h. No silver particles appear on the surface before reaction for the 10% sample. However, after reaction for 2 h, a large number of silver nanoparticles appear on the surface and the particle sizes are in the range of tens to hundreds nanometers. This observation suggests that silver ions are reduced and migrated to the surface from the bulk at the initial stage of the reaction. Therefore, the SEM results are also in good agreement with that of the XRD results. In addition, for a 20 wt% sample (shown in Figs. 3c and d), besides a few silver particles on the surface before reaction, a large amount of silver flakes with sizes at about several hundreds nanometers paved on the surface orderly and almost no support could be observed, demonstrating the unique structure of the surface metallic silver for the reaction. Thus the superior catalytic performance of this novel catalyst system may be attributed to the structural difference between the Ag–SiO_2–Al_2O_3 catalyst and the commercial silver catalyst. As for the catalyst loaded with 30% Ag, there are many silver particles on the surface even before reaction with a substantially higher amount of silver particles appearing on the surface of the catalyst after reaction for 2 h, being very similar to that of the 20% one. This suggests the partial reduction of silver

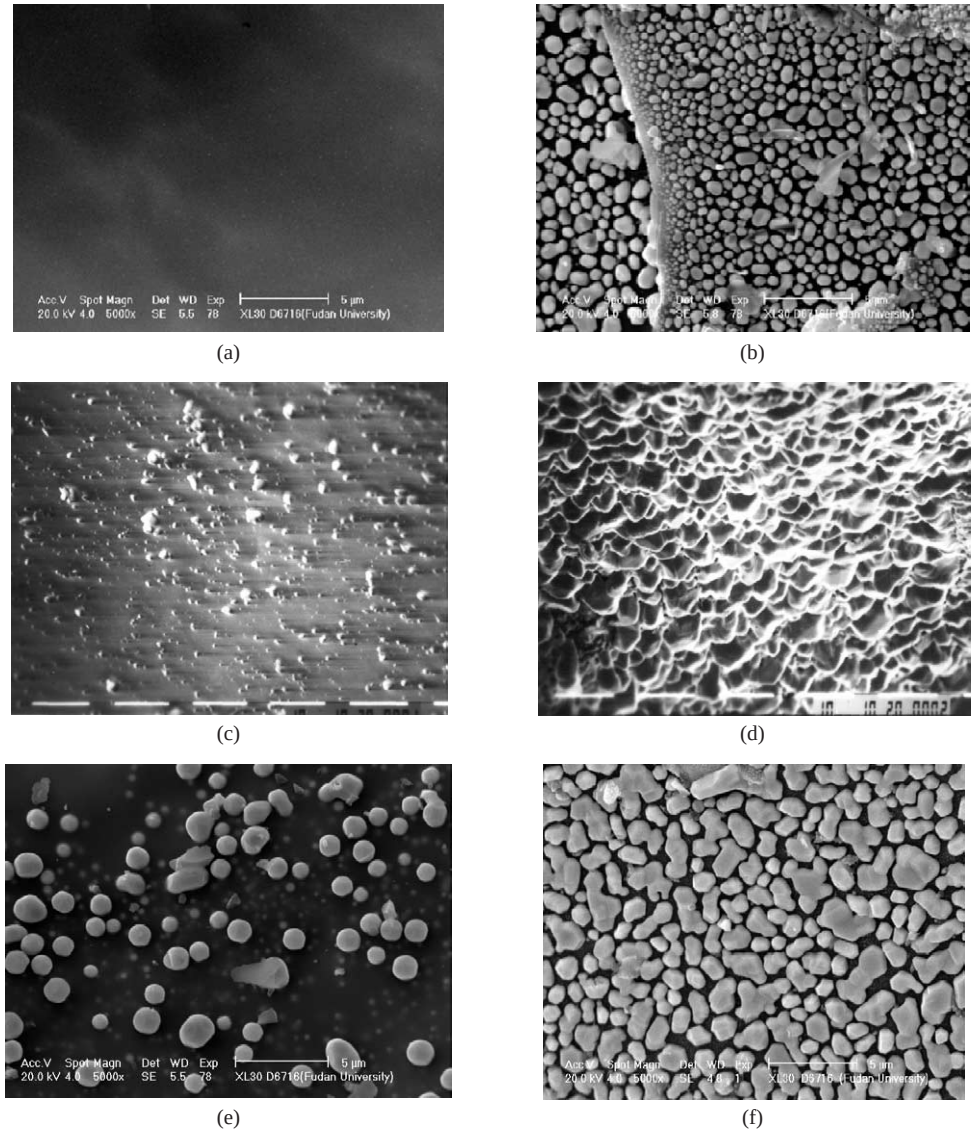

Fig. 3. SEM images of the 10 wt% Ag–SiO_2–Al_2O_3 catalyst before (a) and after reaction for 2 h (b); 20 wt% Ag–SiO_2–Al_2O_3 catalyst before (c) and after reaction for 2 h (d); 30 wt% Ag–SiO_2–Al_2O_3 catalyst before (e) and after reaction for 2 h (f).

and subsequent migration of metallic silver to the surface after the initial period of the reaction. According to SEM results of the three catalysts with different silver loading as shown above, one can conclude that the surface silver concentration is much higher than that of the fresh samples. In addition, when silver loading is lower than 20%, almost no silver particles could be observed on the surface, indicating that silver is fully incorporated in the lattice of the fresh catalyst. If the silver loading is higher than 20%, a substantial amount of metallic silver particles present on the surface, which is much different from that of the 10 and 20% ones, implying that the silver loading of 20% may be a critical point.

From the SEM results, we can also find that there are significant differences in the morphology of the Ag–SiO_2–Al_2O_3 catalyst before and after the initial reaction for 2 h. After that, the morphology does not change anymore. The fact that the surface morphology could be maintained for such a long time reaction even up to 140 h after a 2-h induction period correlates well with the steady performance of the catalyst during the lifetime test. Hence, the morphology of the real active species was suggested to be the isolated metallic silver particles as shown in Figs. 3b, d, and f for the used samples. Thus, the fresh as-calcined samples could be viewed as the precursors for the working catalysts.

3.2.6. TPR

The reduction process of the Ag–SiO_2–Al_2O_3 catalysts with different silver loadings was investigated by using a TPR technique. Fig. 4 presents the TPR profiles of standard Ag_2O sample and a series of Ag–SiO_2–Al_2O_3 catalysts. It is interesting to find that all TPR profiles of the Ag–SiO_2–Al_2O_3 catalysts present much broader and more

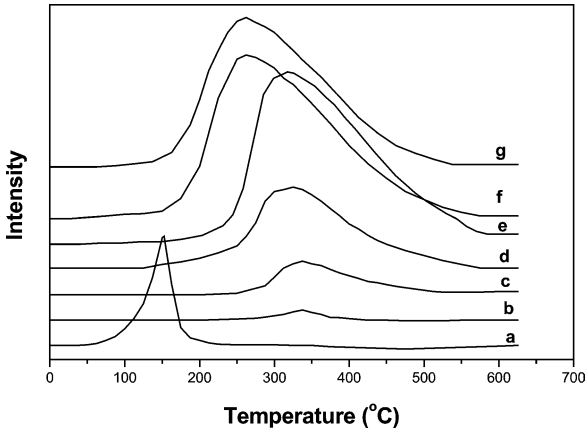

Fig. 4. TPR curves of the standard Ag_2O (a), and the Ag–SiO_2–Al_2O_3 catalysts with silver loading of 1% (b), 2% (c), 10% (d), 20% (e), 30% (f), and 40% (g).

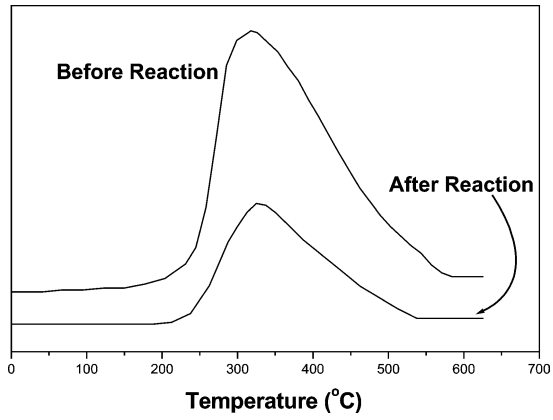

Fig. 5. TPR curves of the 20 wt% Ag–SiO_2–Al_2O_3 catalyst before and after reaction for 2 h.

asymmetric than the Ag_2O one. The reduction temperature of the Ag–SiO_2–Al_2O_3 catalysts is much higher than that of Ag_2O, suggesting that Ag^+ species located in the cavity of the framework of SiO_2–Al_2O_3 is different from that in Ag_2O [19]. In addition, the reduction temperature decreases with increasing of the silver loading, indicating that Ag^+ is easier to be reduced with increasing silver content. Furthermore, for the samples with silver loadings lower than 20 wt%, H_2 consumption is found to be in excellent linear correlation with the silver content based on the quantitative calculation of the TPR peak area. When the silver content is above 20 wt%, H_2 consumption did not increase further, illustrating that the amount of Ag^+ does not increase in the catalysts with silver content higher than 20%. Fig. 5 shows the TPR curves of the 20% sample before and after reaction for 2 h. It illustrates that no significant difference could be observed except for the decrease of 50% peak area after reaction, suggesting that partial Ag^+ is reduced to a metallic state during the initial stage of the reaction, which is in excellent agreement with the XRD and SEM results presented above.

3.2.7. Chemical analysis

In the chemical analysis experiments, the absolute amount of Ag^+ is determined by selectively dissolving the catalyst in hydrofluoric acid followed by chemical titration with KSCN. It is found that all silver is present as an ionic state at the silver concentration smaller than 20% as shown in Fig. 6a. When the silver concentration exceeds 20%, some silver that could not be stabilized by the tetrahedral $[AlO_4]$ groups is present as a metallic state. The result is similar to the TPR result. The results in Fig. 6a also show that the total amount of silver ($Ag^0 + Ag^+$) is slightly smaller than the total amount of silver added (illustrated as the theoretical Ag in Fig. 6), which can be attributed to the experimental error and the volatile loss of silver during calcinations in which the temperature ($> 950\,^\circ C$) is close to the melting point of bulky silver ($960\,^\circ C$) and higher than the melting point of nano-sized silver particles. Moreover, for those Ag–SiO_2–Al_2O_3 catalysts with silver loadings $\leqslant 20$ wt%, silver is totally present as an ionic state before reaction; however, about 50% silver ions are reduced during the initial period of the reaction for the selective oxidation of methanol to formaldehyde. It is very interesting to identify

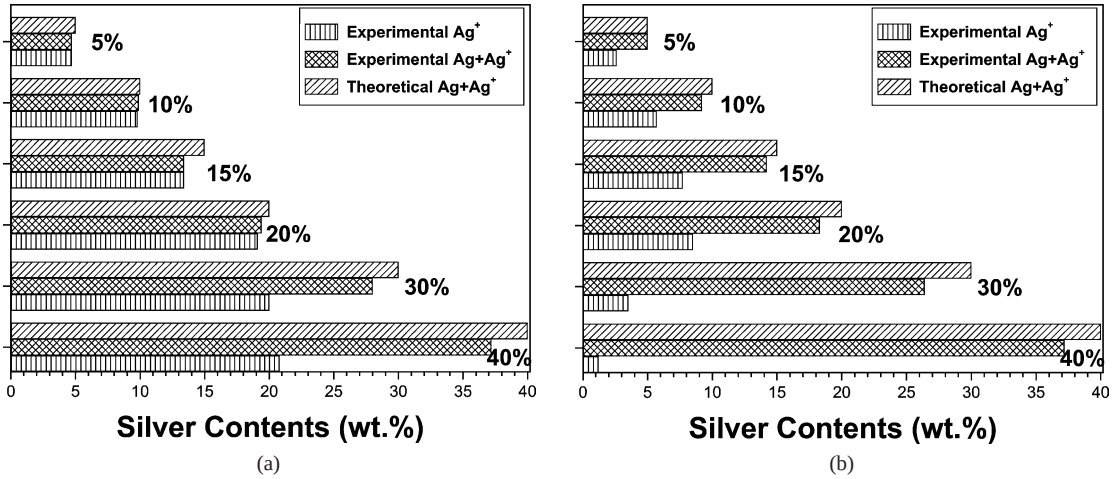

Fig. 6. Ag^0 and Ag^+ contents in Ag–SiO_2–Al_2O_3 catalysts determined by chemical analysis: (a) before reaction; (b) after reaction for 2 h.

that 50% silver changes to the metallic state after reaction for 120 h while the remaining 50% silver still keep its ionic state, which could be explained by considering the reductive atmosphere of the reaction mixture during the selective oxidation of methanol to formaldehyde. As we know, the molar ratio of oxygen to methanol is about 0.4 for the title reaction and there is about 20 vol% H_2 in the tail gas mixture. On the other hand, there is also 29 vol% oxygen in the oxygen–methanol mixture, and the oxygen will react with metallic silver quickly under the reaction conditions (∼ 650 °C). Based on above discussions, there is equilibrium transformation between Ag^+ and Ag^0, and the system containing 50% of metallic silver is the most stable and suitable candidate for the samples containing silver lower than 20% under the reaction conditions. Another interesting result is obtained from Fig. 6b concerned with those samples with silver loadings higher than 20% after reaction for 2 h. The contents of Ag^+ are extremely low and the corresponding catalytic activities are also much lower than their counterparts with silver contents lower than 20%, indicating the importance of the presence of certain amount of Ag^+ during the reaction.

The results of chemical analysis show that the homogeneous glass-like composite of the novel Ag–SiO_2–Al_2O_3 catalyst system can only be obtained with the silver loadings lower than 20%. Also, it is found that the molar ratio of silver to aluminum in the composites is ca. 1:1, suggesting that silver ions could be stoichiometrically stabilized by the [AlO_4] moieties in the homogeneous glass-like composites.

3.2.8. UV–vis DRS

UV–vis DRS is a powerful technique for the investigation of silver-based catalysts. It is commonly accepted that the absorption band at 250 nm is ascribed to the isolated Ag^+, 270 nm to $Ag_n^{\delta+}$, 315–320 nm to metallic silver particles or silver foil, 370–390 nm to microcrystalline silver, and 400–420 nm to silver clusters [20–26]. Fig. 7 shows the UV–vis DRS spectra of 20 wt % samples before and after reaction for 2 h. For the sake of comparison, the UV–vis DRS spectrum of commercial electrolytic silver is also included. There is only one band centered at 250 nm for the sample before reaction, indicating that there are only Ag^+. As to the sample after reaction for 2 h, two additional bands at 315 and 403 nm appear. The former is similar to that of the electrolytic silver, suggesting the presence of large metallic silver particles on the surface, whereas the latter indicates

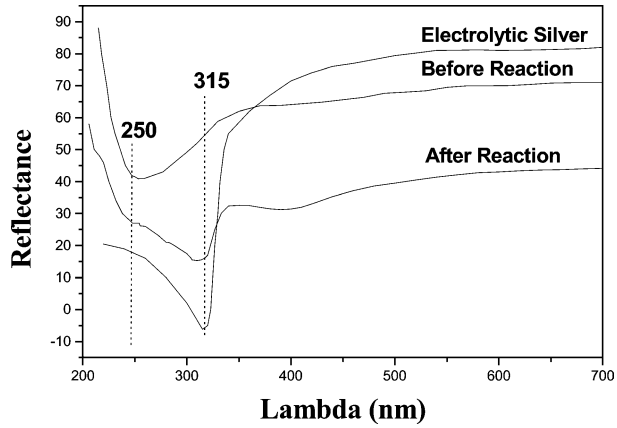

Fig. 7. UV–vis DRS spectra of 20 wt% Ag–SiO_2–Al_2O_3 catalyst before and after reaction for 2 h.

the existence of microcrystalline silver or silver clusters. Other research groups also reported that only one peak at 250 nm assigned to the isolated Ag^+ species was observed with silver content of 10 or 20 wt%, and two bands centered around 315 and 403 nm assigned to the metallic silver particles and silver clusters, respectively, were observed when the silver content exceeded 20 wt% [27,28]. Therefore, the UV–vis DRS spectra unambiguously demonstrate that the Ag^+ ions in the 20 wt% Ag–SiO_2–Al_2O_3 catalyst are partially reduced to metallic silver during the reaction of the selective oxidation of methanol. Obviously, this result is in excellent agreement with the data from the TPR, XRD, and chemical analysis as shown above.

3.2.9. XPS

In order to gain a deeper insight into the effects of silver on the catalytic performance, including the surface content and the electronic properties, a series of Ag–SiO_2–Al_2O_3 catalysts with different preparation conditions were analyzed with XPS.

3.2.9.1. Effect of silver loading. Ag/Si ratios on the surface of all the Ag–SiO_2–Al_2O_3 catalysts with different silver loadings before and after reaction for 2 h determined by XPS are shown in Table 4. It is seen that the surface Ag/Si ratios are far lower than those in the bulk for the catalysts with silver loadings lower than 10% before reaction, which are close to those in the bulk when the silver loadings are in the range of 10–20%. However, if silver loadings are in the range of 20–30%, the surface Ag/Si ratio is slightly higher than that in the bulk. With further increase of silver loadings

Table 4
Influence of silver loading on the surface Ag/Si ratio[a]

S_{Ag}	Silver loading (wt%)									
	0.5	1	2	5	10	12	15	20	30	40
Before reaction	0.27	0.39	0.44	1.37	5.62	9.68	16.5	25.2	33.3	33.5
After reaction	10.2	12.5	42.3	152	198	242	352	383	297	223

[a] Determined as the weight ratio of silver to SiO_2 with XPS. $S_{Ag} = W_{Ag}/W_{SiO_2}$, same as following.

Table 5
Influence of calcination temperature on the surface Ag/Si ratio

S_{Ag}	Calcination temperature (°C)					
	600	700	800	900	1000	1100
Before reaction	19.8	11.9	10.9	3.54	5.62	8.68
After reaction	53.6	51.4	81.9	179	198	152

up to 40%, the value of the surface Ag/Si ratio is similar to that of the 30% Ag–SiO_2–Al_2O_3 sample, implying the saturation of the silver aggregates on the surface. The above results can be explained as follows. Since Ag^+ is stoichiometrically stabilized by the [AlO_4] unit as noted above, it will be dispersed and entered into the most stable region, i.e., the deeper region if the silver loading is very low (< 10%). Therefore, the scattering section area of XPS is very small that may lead to the small surface Ag/Si ratio when determined with XPS. However, with silver loading increasing from 10 to 20%, Ag^+ almost takes up all the most probable positions and disperses homogeneously which brings on the similar value of the surface Ag/Si ratio as that in the bulk. As silver loadings increase progressively from 20 to 30%, the formed metallic silver agglomerates on the surface of the support, thus resulting in the enrichment of silver on the surface. With further increase of silver loading to above 30%, the presence of an excess amount of metallic silver would lead to the rapid growth of the silver particles enriched on the surface, but this does not lead to an increased scattering section area for XPS. Thus, the surface Ag/Si ratio approaches steady when the silver loading is 30% or higher.

For the samples after an initial reaction of 2 h (also shown in Table 4), the surface Ag/Si ratio increases linearly with increasing silver loading if it is lower than 20%. Particularly, the surface Ag/Si ratio reaches 383% for the 20% catalyst. It is remarkable that this value is almost 15 times larger than that of the sample before reaction, suggesting that the surface of the catalyst is almost fully covered by metallic silver particles. SEM photos of the 20% Ag–SiO_2–Al_2O_3 sample before and after reaction for 2 h clearly show significant changes of the surface, thus confirming the conclusion drawn above. It is also very interesting to find that the surface Ag/Si ratio decreases sharply when the silver loading is higher than 20%, probably due to the reason that the silver particles on the surface of these samples may be originated from the rapid growth of the surface silver particles presented before the reaction. In this respect, we believe that the metallic silver presented on the surface before reaction is produced via a pathway different from that generated in situ during the partial oxidation of methanol to formaldehyde. Therefore, the state of the aggregated metallic silver is different between the samples with silver contents higher and lower than 20%. Thus, it is clear that it is difficult to generate a fully silver covered surface during the reaction over the catalyst with silver loadings higher than 20% and the formation of much larger and non-uniform silver particles might be responsible for the correspondingly low catalytic activity.

3.2.9.2. Influence of calcination temperature. Table 5 shows the influence of calcination temperature on the surface Ag/Si ratio of a 10 wt% catalyst before and after reaction for 2 h as measured by XPS. The surface Ag/Si ratio as a function of the calcination temperature for the catalyst before reaction is valley-like, while the one after reaction for 2 h appears to follow a typical volcano shape. Both the maximal and the minimal content values appear at 900–1000 °C, corresponding to the optimal calcination temperature observed in the activity test. It is commonly accepted that the Ag–SiO_2–Al_2O_3 catalysts should be calcined at high temperatures before reaction to remove the surface OH group and to eliminate the microholes by densification of the catalyst. Thus, Ag^+ cannot completely enter into the lattice of the support and will not lead to high surface Ag/Si ratios with low calcination temperatures. On the other hand, under ultrahigh calcination temperatures (> 1100 °C), the typical amorphous structure of the catalyst is destroyed and part of SiO_2 support will be crystallized leading to partial segregation of Ag^+ from the bulk of the catalyst and subsequent aggregation of the silver species on the surface, which may reasonably account for the increment of surface Ag/Si ratio.

The surface Ag/Si ratio of the catalyst after reaction for 2 h is dependent on the reducibility of Ag^+ and the surface structure of the catalyst. For a well-calcined catalyst with a flat and nonporous surface, the reduction of Ag^+ is very slow and silver particles with well-defined structures will aggregate on the surface. Note that calcination temperatures higher or lower than 900–1000 °C favor the irregular separation of Ag^+ on the surface, thus leading to a smaller value of the surface Ag/Si ratio as determined by XPS.

3.2.9.3. Influence of the molar ratio of water/ethanol. Table 6 shows the influence of molar ratio of water/ethanol on the surface Ag/Si ratio of the 10% Ag–SiO_2–Al_2O_3 catalyst before and after reaction for 2 h. The surface Ag/Si ratio of the samples before reaction increases with the increase of water content. After the reaction for 2 h, the sample prepared with a water/ethanol molar ratio of 16 exhibits the maximal surface Ag/Si ratio and the highest catalytic activity in the methanol oxidation. For the catalysts prepared with a water/ethanol molar ratio of 40 or 48, the catalytic activity appears to be rather low, although the surface Ag/Si ratios are still very high. The structural difference of the catalyst may be accountable for this observation. It is found that preparation with high water content may favor the formation of the catalyst with much looser structure, in sharp

Table 6
Influence of molar ratio of water/ethanol on the surface Ag/Si ratio

S_{Ag}	Water/ethanol (molar ratio)					
	8	16	24	32	40	48
Before reaction	2.88	3.93	4.75	3.26	7.78	8.10
After reaction	163	198	155	145	190	192

Table 7
The XPS data of some standard samples

Binding energy (eV)	Sample			
	Ag	Ag_2O	AgO	$AgOOCCF_3$
Ag $3d_{5/2}$	368.3	368.4	368.0	368.8
Ag MNN	358.3	350.6	350.6	355.1

contrast to the glass-like and much compacted structure obtained with low water content.

3.2.9.4. Influence of Si/Al molar ratio. Concerning the 30% Ag–SiO_2–Al_2O_3 catalyst with Si/Al ratio of 8.5/1.5–9/1, there is metallic silver aggregated on the surface before the reaction. As noted above, all the silver may be present as the ionic state and the surface Ag/Si ratio after the reaction for 2 h may reach a much higher value if the Si/Al ratiis changed from 9/1 to 8/2. The result fits what we proposed. For the fresh 30% Ag–SiO_2–Al_2O_3 catalyst with Si/Al ratios of 9/1 and 8/2, the surface Ag/Si ratios are 33.3 and 37.3%, respectively. In comparison, the surface Ag/Si ratios for the catalysts after reaction for 2 h are 329 and 561%, respectively. The latter is the highest value observed in the present work. Therefore, it can be concluded that the higher the Ag^+ content before reaction, the higher the surface Ag/Si ratio after reaction for 2 h.

3.2.9.5. Determination of the chemical state of silver. It is well established that both positions of the core XPS peak—Ag $3d_{5/2}$ and the XAES—Ag MNN can be used to determine the chemical state of the surface silver. XPS results of a number of standard samples are shown in Table 7 for comparison [29]. Similar to that reported previously, it is highly difficult to discriminate the peak position of Ag $3d_{5/2}$ for Ag_2O, AgO, and metallic Ag, thus being impossible to identify the accurate chemical state of silver state only from the analysis of the Ag $3d_{5/2}$ data. Alternatively, the precise chemical state of a specific element could be more easily discriminated by the peak position of XAES, which is much more sensitive to the chemical environment, especially when the corresponding core-level XPS spectra are insensitive to different chemical states. In fact, the peak position of Ag $3d_{5/2}$ in some silver samples also changes appreciably, providing additional opportunity for the analysis of the silver states. Both data of Ag $3d_{5/2}$ and Ag MNN for the catalysts with different silver loading before and after reaction for 2 h are summarized in Tables 8 and 9. It is shown that the difference for the Ag $3d_{5/2}$ position before and after reaction for 2 h decreases with increasing silver loading, possibly due to the reason that Ag^+ is much more stable in the catalyst with low silver loading, thus entailing a high binding energy. From the data listed in Table 8, we can also find that all the binding energies of Ag $3d_{5/2}$ of the supported silver samples are all higher than that of pure Ag_2O and AgO, demonstrating the totally different nature of the silver species as compared to the reference samples. For silver loadings higher than 20%, the presence of loosely aggregated metallic silver particles on the surface of the fresh sample results in the overlapping of the XPS peaks for Ag^+ and Ag species, thus leading to the decrease of the binding energy of Ag $3d_{5/2}$. For Ag MNN, the peak position is difficult to resolve when silver loading is relatively low ($< 5\%$) because of the weak signal. It can also be found that the difference of the Ag MNN position for the samples before and after reaction for 2 h is all above 1.0 eV, suggesting the intrinsically different silver states before and after reaction for 2 h certainly.

Table 8
Position of Ag $3d_{5/2}$ for the Ag–SiO_2–Al_2O_3 catalysts

Binding energy (eV)	Ag loading (wt%)						
	0.5	1	5	10	20	30	40
Before reaction	369.3	369.6	369.3	369.3	368.8	368.9	369.0
After reaction	368.6	368.5	368.3	368.8	368.4	368.8	368.8

Table 9
Position of Ag MNN for the Ag–SiO_2–Al_2O_3 catalysts

Binding energy (eV)	Ag loading (wt%)						
	0.5	1	5	10	20	30	40
Before reaction	–	–	–	350.7	351.3	351.1	350.8
After reaction	352.6	352.1	353.3	352.1	352.8	352.0	352.4

In addition, the Ag MNN XAES values of the catalysts are different from those of metallic silver, or silver oxides (including AgO and Ag_2O), being unique with respect to any known silver-based compounds.

3.3. Discussion

In general, several conclusions may be drawn based on the XPS analysis of the chemical states of silver present on the surface before and after the catalytic reaction. First, silver is present as isolated Ag^+, not Ag_2O and AgO at all, on the surface of the Ag–SiO_2–Al_2O_3 catalysts with silver contents lower than 20%. Batyan et al. also discussed the same issue; however, the catalysts used in their experiments were Kaolin-based silver catalysts and a positive chemical shift about 0.2–0.4 eV in the Ag $3d_{5/2}$ XPS peak was observed [18], smaller than that observed in our present work. The main reason was that there were both metallic and ionic silver present on the surface and might reduce the difference of the BE value for the Ag $3d_{5/2}$ XPS peak. With the Fourier transformation analysis of the EXAFS data, the radial distribution function of silver atoms can be obtained and the maximal value of the peak was 1.96 Å (equivalent to interatomic distance), which is smaller than the $R_{Ag–O}$ of 2.05 Å in Ag_2O and the $R_{Ag–Ag}$ of 2.889 Å in the metallic silver, but is close to that of Al–O (octahedral coordination, $R_{Al–O} =$ 2.0 Å). Hence, the isolated silver ion located in the lattice of the aluminosilicate support surrounded by oxygen atoms is considered to be stabilized [18]. In our present work, a similar effect is also present. Secondly, the silver in the catalyst before reaction (silver content $\leqslant$ 20%) is not present as Ag_2O certainly owing to the results obtained from that of the above characterizations: high thermal stability (> 1000 °C), difference of the XPS peak position of Ag $3d_{5/2}$ and Ag MNN from that of Ag_2O, and the impossibility for the determination of Ag–O vibration by using Raman spectroscopy. Thirdly, the catalysts show an amorphous character before reaction (silver content $\leqslant$ 20%); no crystalline phases could be detected by XRD, indicating the absence of any kinds of Ag^+-incorporated crystalline phases with silicon or aluminum [30]. Based on the fact that the ultimate content of silver ion equals the molar content of aluminum, the possible structure of the catalysts can be proposed as follows. Part of the [SiO_4] groups are replaced by [AlO_4] groups, which create negative charges in the framework. The resulting negative charge can be reasonably balanced by the presence of Ag^+. When the molar content of Ag^+ is lower than Al^{3+}, the [AlO_4] group without a combination of Ag^+ will be present as a microcrystalline phase, which is confirmed by Raman spectroscopy. The reduction process of silver ion to the corresponding metallic silver can be illustrated in Scheme 1, and the regeneration process of the catalyst is the reverse of that shown in Scheme 1. Silver ions can sustain very high temperatures (900–1000 °C) in our catalysts, which is similar to that in the Ag^+-exchanged zeolite. It is known that silver can be easily reduced to a metallic state at temperatures higher than 300 °C. However, in our system, silver can only be present in an ionic state under oxidative atmosphere. When treated under reductive atmosphere, Ag^+ can be partially reduced to metallic species, which is also observed in the selective oxidation of methanol to formaldehyde because the reaction mixture is a typically reductive atmosphere. As illustrated in the scheme shown above, 20% Ag is the upper limit to be stoichiometrically isolated by [AlO_4], regardless of the much small specific area (less than 1 m^2/g) of the support.

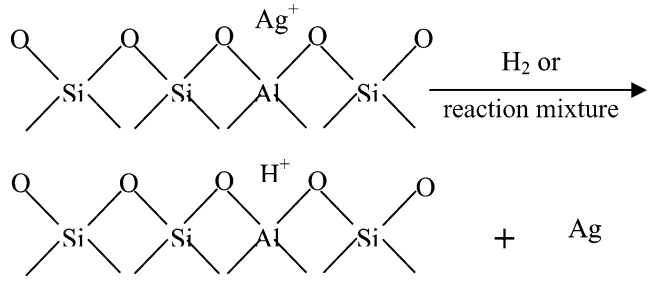

Scheme 1. Possible structure and reduction process of the Ag–SiO_2–Al_2O_3 catalyst.

4. Conclusions

The Ag–SiO_2–Al_2O_3 catalyst prepared by sol–gel method is demonstrated to be a powerful catalyst for the selective oxidation of methanol and the optimal preparation parameters are determined to be the molar ratios of Si/Al of 8.5/1.5–9/1, silver loading of 20%, calcined temperature of 900–1000 °C with ethanol as the solvent. Such catalysts are glass-like and nonporous. For the catalyst with silver loadings lower than 20%, the specific surface area is 1–3 m^2/g and all Ag species are present as Ag^+ ions before catalytic reaction. The catalyst is ultrathermally stable even under temperatures as high as 1100 °C. During reaction, Ag^+ ions are partially reduced to metallic Ag with particle sizes around hundreds nanometers. The catalyst shows excellent stability in methanol oxidation and no appreciable deactivation or structural changes are observed even after reaction for more than 140 h.

After a short induction period, silver is reduced and enriched gradually on the surface during the catalytic reaction, resulting in a dramatically high surface concentration. The catalyst with silver loadings of 20% shows the highest surface Ag/Si ratio and unique surface morphology, which is believed to account for its excellent catalytic performance. Based on various characterizations, it is proposed that Ag^+ is stoichiometrically stabilized by [AlO_4] moieties present in the silica–alumina support. The active centers for the selective oxidation of methanol to formaldehyde over Ag–SiO_2–Al_2O_3 catalyst are considered as nano-sized metallic silver particles copresent with Ag^+.

Acknowledgments

This work was financially supported by the Major State Basic Resource Development Program (Grant 2003CB615807), NSFC (Project 20073009), the Natural Science Foundation of Shanghai Science and Technology Committee (02DJ14021, and the Committee of the Shanghai Education (02SG04).

References

[1] M.V. Twigg, in: Catalyst Handbook, Wolfe, London, 1989, p. 490.
[2] C.A. Bazilio, W.J. Thomas, U. Ullah, K.E. Hayes, Proc. R. Soc. London, Ser. A 399 (1985) 181.
[3] L. Lefferts, H. van Ommen, J.R.H. Ross, J. Chem. Soc. Faraday Trans. 84 (1) (1988) 1491.
[4] L. Lefferts, H. van Ommen, J.R.H. Ross, J. Catal. 114 (1988) 303.
[5] L. Lefferts, H. van Ommen, J.H.R. Ross, Proc. 9th Int. Conf. Catal. 4 (1988) 1672.
[6] M. Qian, M.A. Liauw, G. Emig, Appl. Catal. A 238 (2003) 211.
[7] S. Brandani, V. Brandani, G. Di Giacomo, Ind. Eng. Chem. Res. 31 (1992) 1792.
[8] M.L. Kaliya, G.Yu. Nechaeva, N.V. Kul'kova, Kinet. Katal. 23 (5) (1982) 1287.
[9] S.V. Matveichuk, V.N. Makatun, Dokl. Akad. Nauk. BSSR 28 (8) (1984) 733.
[10] L.A. Manucharova, T.G. Alkhazov, Z. Fiz. Khim. 60 (1986) 73.
[11] T. Lopez, L. Gaona, R. Gomez, J. Noncryst. Solids 110 (1989) 170.
[12] T. Lopez, P. Bosch, M. Asomoza, R. Gomez, J. Catal. 133 (1992) 247.
[13] W.-L. Dai, J.-L. Li, Y. Cao, J.-F. Deng, Catal. Lett. 64 (1) (2000) 37.
[14] Y. Cao, W.-L. Dai, J.-F. Deng, Mater. Lett. 50 (1) (2001) 12.
[15] W.-L. Dai, Y. Cao, H.-X. Li, J.-F. Deng, Chem. Lett. 3 (1997) 197.
[16] Y. Cao, W.-L. Dai, J.-F. Deng, Appl. Catal. A 158 (1997) 27.
[17] W.-L. Dai, Q. Liu, Y. Cao, J.-F. Deng, Appl. Catal. A 175 (1998) 83.
[18] E.Yu. Batyan, S.V. Mateveichuk, G.A. Branitskii, Kinet. Catal. 136 (1995) 816.
[19] B. Pettinger, X.H. Bao, I. Wilcock, M. Muhler, R. Schlogl, G. Ertl, Angew. Chem. Int. Edit. 33 (1) (1994) 85.
[20] W.N. Delgass, in: Spectroscopy in Heterogeneous Catalysis, Academic Press, New York, 1979, p. 86, Chapter 4.
[21] L.R. Gellens, R.A. Schoonheydt, in: P.A. Jocobs (Ed.), Metal Microstructure in Zeolites, Elsevier, Amsterdam, 1982, p. 87.
[22] H.E. Rhodes, P.-K. Wang, H.T. Stokes, C.P. Slichter, J.H. Sinfelt, Phys. Rev. 1326 (1982) 3559.
[23] H.E. Rhodes, P.-K. Wang, C.D. Makowka, S.L. Rudaz, C.P. Slichter, J.H. Sinfelt, Phys. Rev. 1326 (1982) 3569.
[24] H.T. Stokes, H.E. Rhodes, P.-K. Wang, C.P. Slichter, J.H. Sinfelt, Phys. Rev. 1326 (1982) 3575.
[25] I. Yu, A.A. Gibson, R.E. Hunt, W.P. Halperin, Phys. Rev. Lett. 44 (1980) 348.
[26] G.K. Boreskov, in: Heterogeneous Catalysis, Nauka, Novosibirsk, 1988 (in Russian).
[27] J. Texier, J.J. Hastrelter, J.L. Hall, J. Phys. Chem. 87 (1983) 4690.
[28] N. Pestryakov, A.A. Davydov, J. Electron Spectrosc. 74 (1995) 195.
[29] C.D. Wagner, W.M. Riggs, L.E. Davis, J.F. Moulder, in: G.E. Muilenberg (Ed.), Handbook of X-Ray Photoelectron Spectroscopy, Perkin–Elmer Corporation, 1979.
[30] S. Yuvaraj, S.C. Chow, C.T. Yeh, J. Catal. 198 (2) (2001) 187.